Long-Service-Life Rigid Polyurethane Foam Fillings for Spent Fuel Transportation Casks

Zhenyu Zhang , Guangyao Shen , Rongbo Li , Lei Yuan , Hongfu Feng , Xiuming Chen , Feng Qiu * , Guangyin Yuan * , Xiaodong Zhuang *

Posted Date: 21 December 2023

doi: 10.20944/preprints202312.1599.v1

Keywords: polyurethane foam; fillings; long-service life; spent fuel; flame retardance

Article

Long-Service-Life Rigid Polyurethane Foam Fillings for Spent Fuel Transportation Casks

Zhenyu Zhang [1,2], Guangyao Shen [2], Rongbo Li [2], Lei Yuan [3], Hongfu Feng [2], Xiuming Chen [2], Feng Qiu [4,*], Guangyin Yuan [1,*] and Xiaodong Zhuang [3,*]

[1] National Engineering Research Center of Light Alloy Net Forming & State Key Laboratory of Metal Matrix Composite, Shanghai Jiao Tong University, 800 Dongchuan Road, Shanghai, 200240, China
[2] Shanghai Nuclear Engineering Research and Design Institute Co., Ltd. 169 Tianlin Road, Xuhui District, Shanghai 200030, China
[3] The Meso-Entropy Matter Lab, State Key Laboratory of Metal Matrix Composites & Shanghai Key Laboratory of Electrical Insulation and Thermal Ageing, Frontiers Science Center for Transformative Molecules, School of Chemistry and Chemical Engineering, Shanghai Jiao Tong University, 800 Dongchuan Road, Shanghai 200240, China
[4] School of Chemical and Environmental Engineering, Shanghai Institute of Technology, 100 Haiquan Road, Shanghai 201418, China
* Correspondence: fengqiu@sit.edu.cn (F.Q.); gyyuan@sjtu.edu.cn (G.Y.) zhuang@sjtu.edu.cn (X.Z.)

Abstract: Soft materials bearing rigid, lightweight, and vibration-dampening properties offer distinct advantages over traditional wooden and metal-based fillings for spent fuel transport casks, due to their low density, tunable structure, excellent mechanical properties, and ease of processing. In this study, a novel type of rigid polyurethane foams is prepared using a conventional polycondensation reaction between isocyanate and hydroxy groups. Moreover, the density and size of the pore in these foams are precisely controlled through simultaneous gas generation. The as-prepared polyurethane exhibits high thermal stability exceeding 185 °C. Lifetime predictions based on thermal testing indicate that these polyurethane foams could last up to over 60 years, which is double lifetime of conventional materials of about 30 years. Due to their occlusive structure, the mechanical properties of these polymeric materials meet the design standards for spent fuel transport casks, with maximum compression and tensile stresses of 6.89 and 1.37 MPa, respectively, at a testing temperature of -40 °C. In addition, these polymers exhibit effective flame retardancy; combustion ceased within 2 s after removal of the ignition source. All in all, this study provides a simple strategy for preparing rigid polymeric foams, presenting them as promising prospects for application in spent fuel transport casks.

Keywords: polyurethane foam; fillings; long-service life; spent fuel; flame retardance

1. Introduction

Amid growing concerns regarding global environmental protection, countries are seeking alternative energy sources that do not emit greenhouse gases to replace fossil fuels. In the meantime, the Nino phenomenon exacerbates electricity shortages [1-2]. Currently, renewable energy sources can be divided into solar, wind, and geothermal energy, nuclear power, etc. Among them, nuclear power has much received attention for its high energy density and consistent electricity output[3]. As of now, more than 400 nuclear power reactors are either under operation or under construction worldwide, with the global installed capacity expected to reach 394 million kW[4]. An aspect of the use of nuclear energy is the management of spent fuel, which emits strong hazardous neutron- and gamma-ray radiations. The proper and safe disposal of spent fuel is an unavoidable challenge for the sustained usage of nuclear power [5]. Several countries, including France, China, and Russia, choose the "post-treatment" strategy. In this approach, spent fuel in stored in specialized facilities until its radioactivity reduces sufficiently for reprocessing[6]. The safe transportation of this spent fuel

 doi:10.20944/preprints202312.1599.v1

requires specialized casks designed to shield against radioactivity, which incorporates multiple layers of materials such as steels, lead, concretes, and polymers[7-9]. However, the loading capacity of these specialized cask is much lower than that of traditional containers. Thus, the lightweight design and construction of transportation casks for spent fuel storage remain great challenges.

The spent fuel cask is mainly composed of an outer shell, an anti-vibration layer, a fuel assembly featuring a neutron absorber, and a moderator plate [10]. Among these, the anti-vibration layer occupies a substantial volume in the cask and serves multiple purposes: vibration dampening, buffering, heat insulation, and fire resistance[11]. Generally, timber and honeycomb aluminium are used as anti-vibration materials. However, the energy absorption characteristics of these materials are greatly affected by orientation owing to their intrinsic anisotropy properties[12-13]. Polymeric foams are lightweight materials with the advantages of low cost, tunable structure, ease of processing, and multifunctionality. These materials are commonly used in automotive engineering, thermal insulation, acoustic dampening, biomedical applications, energy storage solutions, and sensor technologies[14-18]. Rigid polyurethane foam, a type of thermosetting polymer resin, has shown promise as a shock absorption layer filling material[19]. Moreover, with a rising strain rate, the energy absorption capability of polyurethane foam increases markedly, and the material becomes stiffer, making it a suitable candidate for the construction of spent fuel transportation casks[20]. However, its anti-vibration performance depends on its density, which consequently affects its weight. Thus, optimizing the trade-off between the anti-vibration performance and weight of rigid polyurethane foam is highly desirable. To the best of our knowledge, few studies have reported on the rational preparation of rigid polyurethane foam as an anti-vibration filling material that would ensure the safety of new spent fuel transport casks. Moreover, scant literature exists on predicting the service lifetime of rigid polyurethane foam through a reliable thermal aging approach.

In this study, rigid polyurethane foams (RPUF) with different densities and pore sizes were synthesized using a conventional foaming technique. This process involved a reaction between isocyanate and hydroxy groups. The elemental compositions and structures of these rigid polyurethane foams were well-characterized by elemental analysis (EA) and Fourier-transform infrared (FTIR) spectroscopy. The morphological and mechanical performance of the foams can be effectively modulated by adjusting the material density. These foams exhibited low water absorption and effective flame-retardant properties. Thermogravimetric analysis revealed that the service lifetime of the rigid polyurethane foam is more than 66 years, which meets the design requirements for properly protecting the fuel assembly. This study provides a new path for the development of rigid polyurethane foams with robust mechanical properties, which are suitable for use in spent fuel transportation casks.

2. Materials and Methods

2.1. Materials

Dihydroxy polyether glycol (PEG-$(OH)_2$, Mn = 600), methylene diphenyl diisocyanate (MDI), dimethyl methanephosphonate, polysilane, and triethanolamine were purchased from Aladdin Reagent and used without purification.

2.2. Preparation procedure

The rigid polyurethane foams were prepared using the in-situ foaming method. A mixture of PEG-$(OH)_2$, dimethyl methane phosphonate, distilled water, triethanolamine, and polysilane with the weight ratio of 100:40:0.6:2:0.8 was stirred in a container at 30 °C. Then, this mixture and MDI with molar ratio of 1:1 were added in a mould quickly (in 10 s), and left them for 18 h to achieve the high-density RPUF (HD-RPUF) material.

For preparation of middle-density RPUF (MD-RPUF), the weight ratio of PEG-$(OH)_2$, dimethyl methanephos-phonate, distilled water, triethanolamine, and polysilane in the mixture was 100:40:2.6:2:0.8.

 doi:10.20944/preprints202312.1599.v1

For preparation of low-density RPUF (LD-RPUF), the weight ratio of PEG-$(OH)_2$, dimethyl methanephos-phonate, distilled water, triethanolamine, and polysilane in the mixture was 100:40:3.4:10:0.2.

2.3. Characterization

Fourier Transform Infrared Spectroscopy (FTIR) spectra were recorded on a Spectrum 100 spectrometer (Perkin Elmer) with KBr powder. The elemental composition was tested by elemental analysis (FlashSmart CHNS, Thermo Fisher). Thermo gravimetric analysis (TGA) spectra were performed on a thermogravimetric analyzer (Q5000IR, TA) under N_2 atmosphere from 25 to 600 °C with 20 °C min^{-1}. Differential scanning calorimetry (DSC) spectra were received from a DSC 6000 spectrometer (Perkin Elmer) under N_2 atmosphere for two heating/cooling cycling from -50 to 180 °C with 10 °C min^{-1}. Scanning electron microscope (SEM) images was obtained from an Sirion-200 field-emission SEM equipment (Field Electron and Ion Company (FEI Co.), USA). The compression and tensile tests were carried out at testing machine (EMIC Corp. model DL2000) following the standard ASTM D 695-15 and ASTM D412, respectively. Aging prediction test was performed by TGA analysis from room temperature to 500 °C with different heating rate of 5, 10, 15, and 20 K min^{-1} under the air atmosphere.

3. Results

The rigid polyurethane foams in this study were synthesized using dihydroxy poly(ether polyol) (PEG-$(OH)_2$) and 4,4'-methylenediphenyldiisocyanate (MDI) as monomers. The synthesis employed a typical polycondensation method and incorporated dimethyl methane phosphonate as a flame retardant, distilled water as a foaming agent, polysilane as a defoaming agent, and triethanolamine as a catalyst[21]. To improve the thermal aging properties of the polymers, silver nitrate is added to reduce halogen content. During the polymerization process, the monomers rapidly combine, resulting in a volume increase. The volume of the polyurethane foam also expands in correlation with the increased concentration of the foaming agent, which in turn affects the density of these foams. The densities of the as-prepared polyurethane foams are 0.32, 0.16 and 0.10 g cm^{-3}, respectively. Correspondingly, these foams are also designated as HD-RPUF, MD-RPUF, and LD-RPUF. The detailed preparation methods for these polyurethane foams are given in the section of "Materials and Methods".

The structural characteristics of these polyurethane foams were elucidated using FTIR. As depicted in **Figure 1**, all the samples yield similar spectral profiles. The peaks locate at wavenumbers of 1729, 1619, and 1223 cm^{-1} corresponded to C=O stretching vibrations, C-O stretching in carbonyl groups, and C-N bonds, respectively. These peaks indicate the existence of the urethane main linkage in the as-prepared polyurethanes. In addition, the peak at 3434 cm^{-1} corresponds to the N-H bond in urethane[22]. For the monomer of poly(ether polyol), the O-C-O stretching peak appears at 1089 cm^{-1}[23]. The C=C bonds related to the aromatic groups in the MDI monomer are found at 1660 cm^{-1}[24]. These results indicate the successful synthesis of rigid polyurethanes foams using PEG and MDI. Elemental analysis further validated the structural characteristics with the results listed in **Table 1**. These results indicate that the three types of polyurethane foams have similar elemental compositions of C, N, and O; generally, chlorine, which may generate free radicals that reduce the service life of the material, is present in low amounts. Herein, all of synthesized materials have low chlorine content, suggesting their favorable thermal aging performance when used in spent fuel transportation casks.

Table 1. Element content and flame retardancy properties of as-prepared polyurethane foams.

Sample	Contents of elements (wt%) [a]								Flame extinction time (s)	Residual carbons (wt%) [b]
	C	H	N	O	P	Si	Cl	Other		

Preprints (www.preprints.org) | NOT PEER-REVIEWED | Posted: 21 December 2023 doi:10.20944/preprints202312.1599.v1

HD-RPUF	61.82	6.04	7.13	14.7	1.125	0.078	0.005	<1	0.88	96.71±1.70%
MD-RPUF	62.73	6.13	7.27	13.6	0.905	0.088	0.005	<1	1.08	92.48±0.77%
LD-RPUF	62.51	6.07	7.36	13.2	1,736	0.021	0.004	<1	1.26	90.64±1.44%

[a)] elemental composition tested by elemental analysis measurement; [b)] ratio of weight after the flame tests.

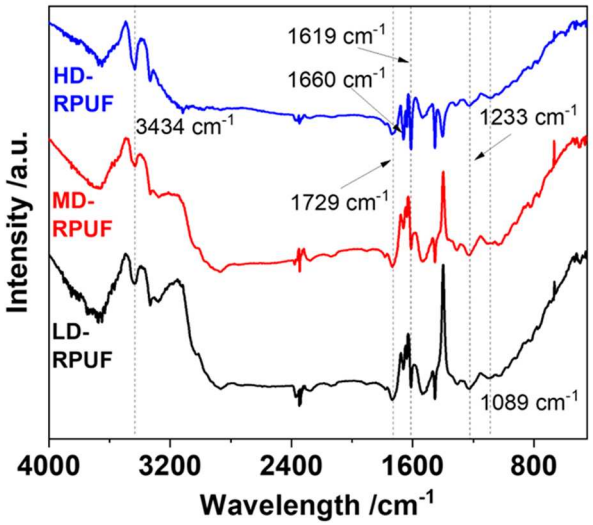

Figure 1. FTIR spectra of HD-RPUF, MD-RPUF and LD-RPUF.

The density of as-prepared foams is highly dependent on their pore size. The morphologies of as-prepared foams were characterized using a scanning electron microscope (SEM; **Figure 2a–c**). The SEM images reveal numerous spherical cells with similar obturator structure, indicating they are typical rigid polymeric foams[25]. An enlarged view in Figure 2b clearly displays that these ruptured microspheres have internal hollow spaces, indicating the porous cell structure of the foams. The choice of foaming agent greatly influences the structure of these hollow microspheres. As the water content in the reactant increases, the diameter of these microspheres increases from 0.185 to 0.415 mm (**Figure 2d**) due to the decrease in interfacial free energy of the pore during the polymerization process[26]. Moreover, an increase in water content leads to greater polydispersity in the diameter distribution and introduces discontinuities between the microspheres

Preprints (www.preprints.org) | NOT PEER-REVIEWED | Posted: 21 December 2023 doi:10.20944/preprints202312.1599.v1

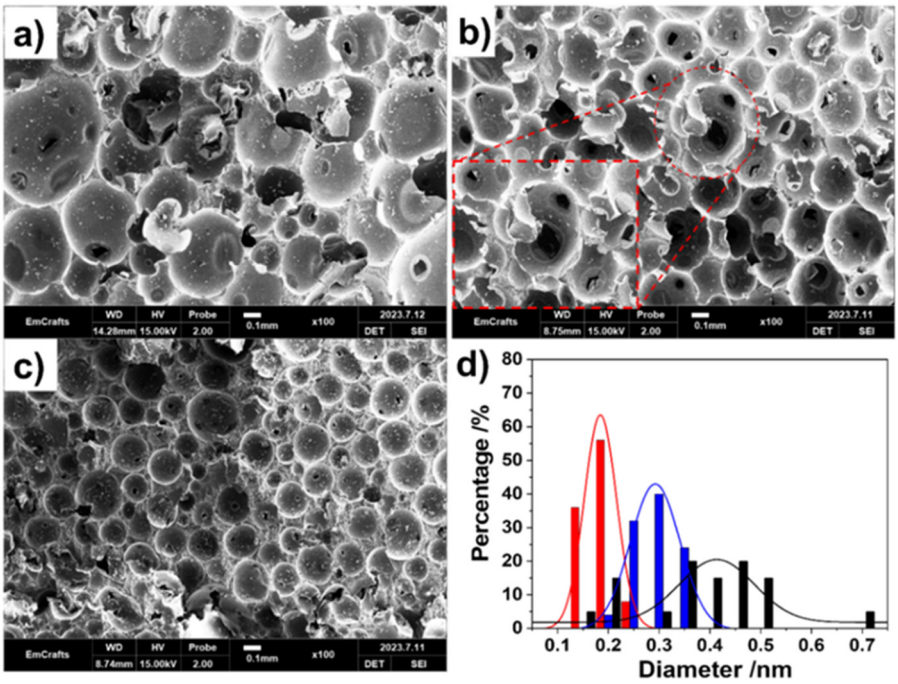

Figure 2. SEM images of LD-RPUF (a), MD-RPUF (b) and HD-RPUF(c); size distribution of cells in LD-RPUF, MD-RPUF and HD-RPUF, respectively.

The thermal stability of these rigid polyurethane foams was measured at a rate of 10 K min^{-1} in nitrogen atmosphere. As depicted in **Figure 3a**, these polyurethane foams exhibit favorable thermal stability up to 400 °C. The temperatures corresponding to a 5% weight loss for LD-RPUF, MD-RPUF, and HD-RPUF are 192.2, 190.3, and 187.0 °C, respectively. Notably, nearly 2% of the thermal weight loss in all three polyurethane foams is attributed to water evaporation from the foam pores, which occurs at approximately 150 °C[27]. These results indicate that the as-prepared polyurethanes exhibit stable thermal properties at room temperature. The rapid thermal degradation of these foams occurs in the range of 305 to 350 °C, which is attributable to the breakage of the main urethane chains, leading to similar decomposition temperatures[28]. Moreover, 21–31 wt% of residual carbon remains after thermal degradation at temperatures exceeding 600 °C, indicative of their highly cross-linked structure and MDI content.

The differential scanning calorimetry thermographs of the rigid polyurethane foams are presented in **Figure 3b-d**. In the first heating cycling, melting endotherm peaks in the range of 63 °C to 70 °C are associated with the crystalline regions formed by the ordered soft polyether and hard MDI segments, which are formed through hydrogen bonds and π-π interactions, respectively. Such broad melting peaks indicate polydispersity in the size and distribution of these crystalline regions[29]. Moreover, the melting point of HD-RPUF is higher than those of MD-RPUF and LD-RPUF, suggesting that the denser structure restricts heat transfer through the polyurethane foam. Due to the foam's rigid structure, ordered structures form slowly, resulting in the absence of a crystalline peak during the second heating cycling. Consequently, the glass transition temperature (T_g) for HD-RPUF is higher than that for MD-RPUF and LD-RPUF.

Preprints (www.preprints.org) | NOT PEER-REVIEWED | Posted: 21 December 2023 doi:10.20944/preprints202312.1599.v1

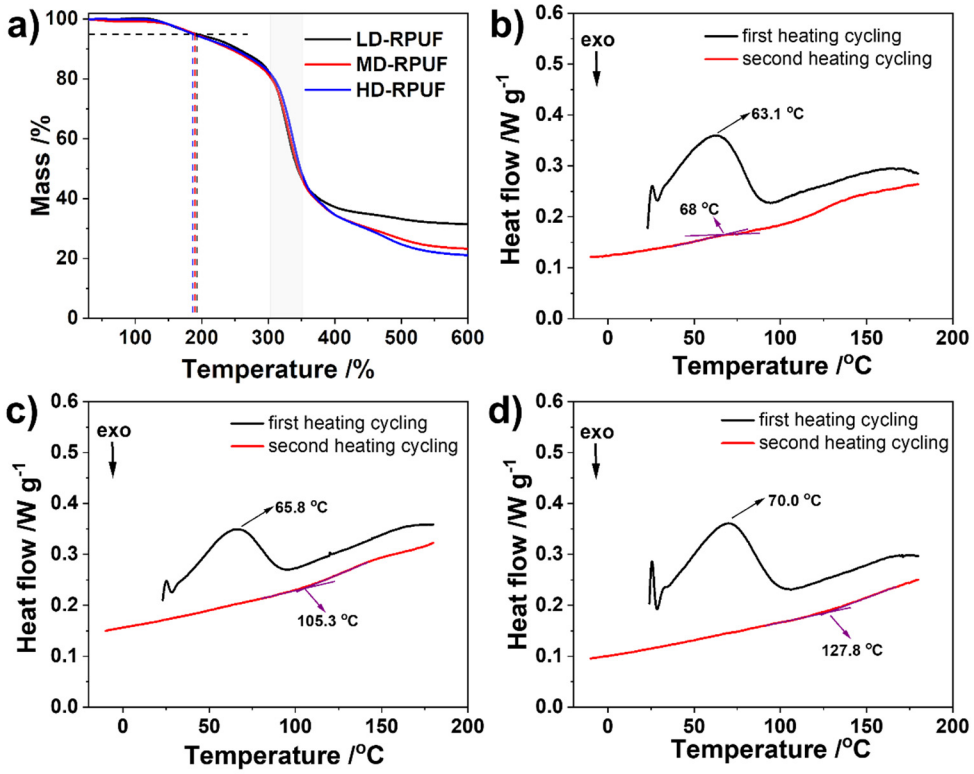

Figure 3. TGA curves of LD-RPUF, MD-RPUF and HD-RPUF in a nitrogen atmosphere; DSC curves of LD-RPUF(b), MD-RPUF(c) and HD-RPUF(d), respectively, under a nitrogen atmosphere.

To simulate the operating temperature of rigid polyurethane foams, mechanical tests were conducted at temperatures of −40, 25, and 70 °C. For compression testing, all samples were initially shaped into cubes with width × length × height of 100 × 100 × 50 mm, respectively. **Figure 4a–c** illustrate that the material volume decreases under applied stress. Using the maximum stress under 10% strain as an indicator of impact resistance, the recorded values for LD-RPUF, MD-RPUF, and HD-RPUF at −40 °C were 6.89, 1.59, and 0.52 MPa, respectively. These values meet the design requirements for compression stress in spent fuel transport tanks, which is attributable to their occlusive structure and rigid polymeric backbone, such as MDI. As expected, HD-RPUF, having the highest density, also exhibits the highest compression resistance. These trends are consistent at test temperatures of 25 and 70 °C. According to classical polymer physics, molecular chain and segment mobility in the material increase with rising temperature. Moreover, according to the DSC results, the melting of crystalline domains in the polyurethane foam occurs at temperatures above 25 °C, leading to reduced compressibility[30]. For example, as the temperature shifted from −40 to 70 °C, the compression stress in HD-RPUF was reduced to 2.43 MPa, indicating the softening of the polyurethane foams at higher temperatures.

For the tensile test, the representative stress–strain curves of LD-RPUF, MD-RPUF, and HD-RPUF are shown in **Figure 4d–f**. For example, when tested at −40 °C, the stress–strain curves for these materials initially exhibited a linear increase at low strain, suggesting typical elastic deformation. As the strain continued to increase, the stress increases sharply until fracture, which is attributable to both the deformation of crystallization domains and the alignment of structural backbone[31]. The tensile stress for HD-RPUF is 1.37 MPa, exceeding those of MD-RPUF (0.51 MPa) and LD-RPUF (0.31 MPa). However, the maximum strain increases with the decreasing of density of polyurethane foam. This phenomenon suggests that foams with larger pore sizes exhibit excellent stretchability under stress, leading to greater material strain. When the test temperature increases, HD-RPUF displays the highest elongation at fracture, whereas LD-RPUF exhibits the highest tensile strain. In addition, tensile values at the point of elongation remain stable at different testing temperatures, indicating that material fracture is highly dependent on the inherent intermolecular interaction of polymer

Preprints (www.preprints.org) | NOT PEER-REVIEWED | Posted: 21 December 2023 doi:10.20944/preprints202312.1599.v1

chains. Conversely, elongation strains at the point of fracture extend as test temperatures increase[32], which can be attributed to enhanced the molecular chain and segment mobility of the material.

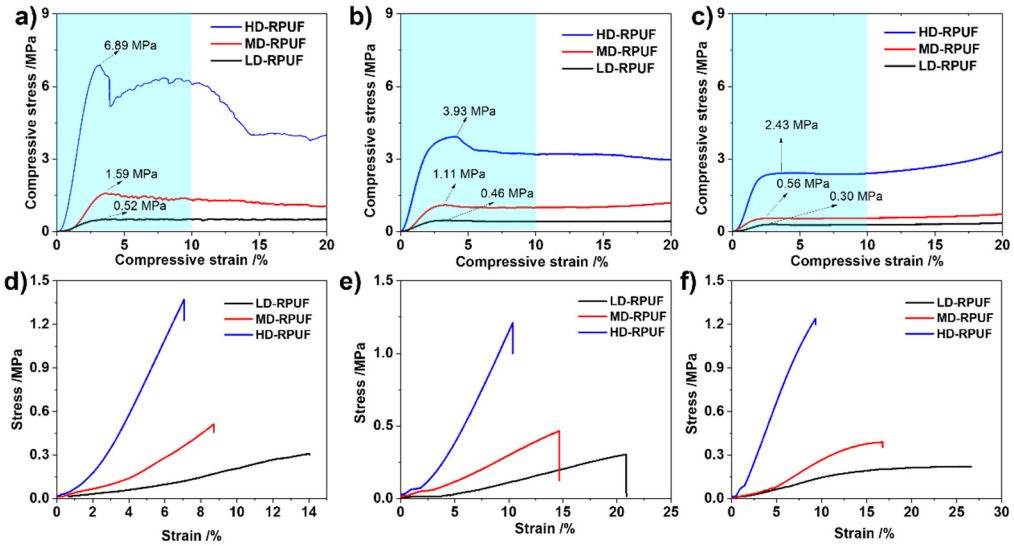

Figure 4. Compression stress-strain curves of LD-RPUF, MD-RPUF and HD-RPUF under the testing temperature of −40 °C (a), 25 °C (b), 70 °C (c); Tensile stress-strain curves of LD-RPUF, MD-RPUF and HD-RPUF under the testing temperature of −40 °C (d), 25 °C (e), 70 °C (f).

Owing to the similar thermal stabilities of the as-prepared materials, the lifetime of these polyurethane foams was evaluated using thermal aging tests, with LD-RPUF serving as the model. **Figure 5a** displays the thermogravimetric analysis (TGA) curves illustrating the thermal decomposition of LD-RPUF from room temperature to 500 °C under the different heating rates, including 5, 10, 15, and 20 K min^{-1}. In **Figure 5a**, these polyurethane foams exhibit stable thermal properties at <150 °C in an air atmosphere. Rapid degradation occurs at temperatures exceeding 300 °C, a threshold is lower than that observed in a nitrogen atmosphere; this may be attributable to accelerated oxidation in the existence of oxygen. As the heating rate increases, the rate of thermal degradation of LD-RPUF decreases, which is likely due to the heat diffusion hysteresis phenomenon in the material[32].

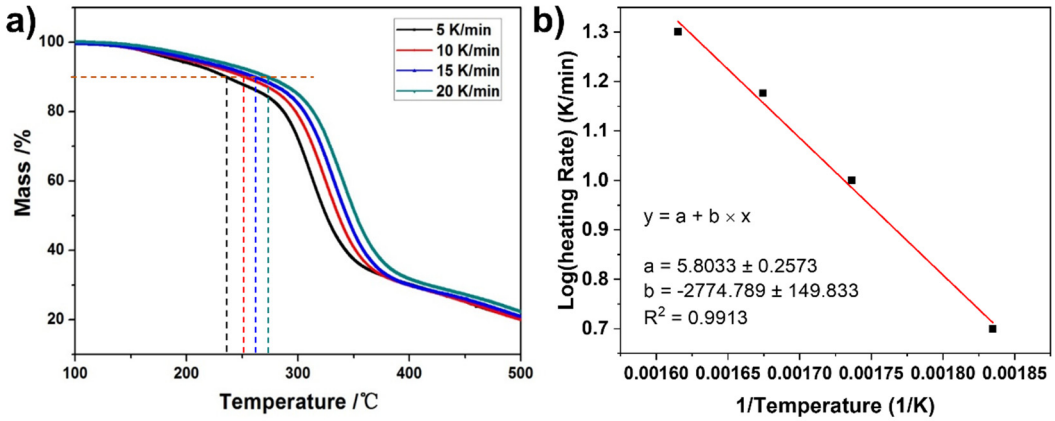

Figure 5. TGA curves of LD-RPUF at different heating rates (a); Linear fitting of the TGA results.

Using 10% weight loss in the TGA as the failure criterion[33], the $T_{10\%}$ temperatures for LD-RPUF in kelvin are 545.03 K, 575.94 K, 597.17 K, and 619.15 K at the heating rates of 5, 10, 15, and 20 K min^{-1}, respectively. The relationship between the logarithm of the heating rates (log β) and the reciprocal of $T_{10\%}$ (1/T) is given in **Figure 5b**. The fitted line exhibits a strong linear correlation. the coefficient of

Preprints (www.preprints.org) | NOT PEER-REVIEWED | Posted: 21 December 2023 doi:10.20944/preprints202312.1599.v1

determination (R2) of 0.9913 is obtained[34]. The Flynn–Wall–Ozawa equation was employed to calculate the apparent activation energies of polymeric materials in accordance with the ASTM E1641-07 standards[35]. The equation is defined as follows:

$$E = -(R/b) \times \Delta(\log \beta)/\Delta(1/T) \quad , \tag{1}$$

where R is the universal gas constant (8.314 J mol−1 · K−1), b is a differential approximation, and $\Delta(\log\beta)/\Delta(1/T)$ is the slope of the logarithm of the heating rates and the reciprocal of $T_{10\%}$. Activation energy (E) of 104.89 kJ mol−1 is obtain by calculation of equation (1).

Thus, the predicted lifetime of LD-RPUF can be obtained using the ASTM E1877 standards and is given by the following equation:

$$\log t_f = E/\left(2.303RT_f\right) + \log[E/(R\beta)] - a, \tag{2}$$

where t_f is the service lifetime, T_f is the service temperature, and a is an integral approximation.

At the maximum service temperature of 30 °C, the predicted lifetime of the LD-RPUF foam is 95 years. Thus, the actual service lifetime of these polyurethane foams would be 66 years according to the safety coefficient of 0.7, which exceeds the standard service lifetime of 30 years for spent fuel transport casks.

Flame retardancy tests were conducted for the as-prepared polyurethane foams, with the results summarized in **Table 1** and **Figure 6**. After ignition, flames spread rapidly across the material surfaces, accompanied by black smoke. Digital photos taken during tests reveal no evidence of melt dripping from the as-prepared polyurethane foams. Once the ignition source is removed, the combustion of the as-prepared materials ceases quickly before complete carbonization could occur. **Figures 6d–f** indicate that the combustion of these polyurethane foams ceases within 2 s, suggesting that phosphonate compounds effectively prevent re-ignition during the flame tests[36]. Moreover, the carbon residue ratios exceeded 90%, further demonstrating the high flame-retardant efficiency of these rigid polyurethane foams.

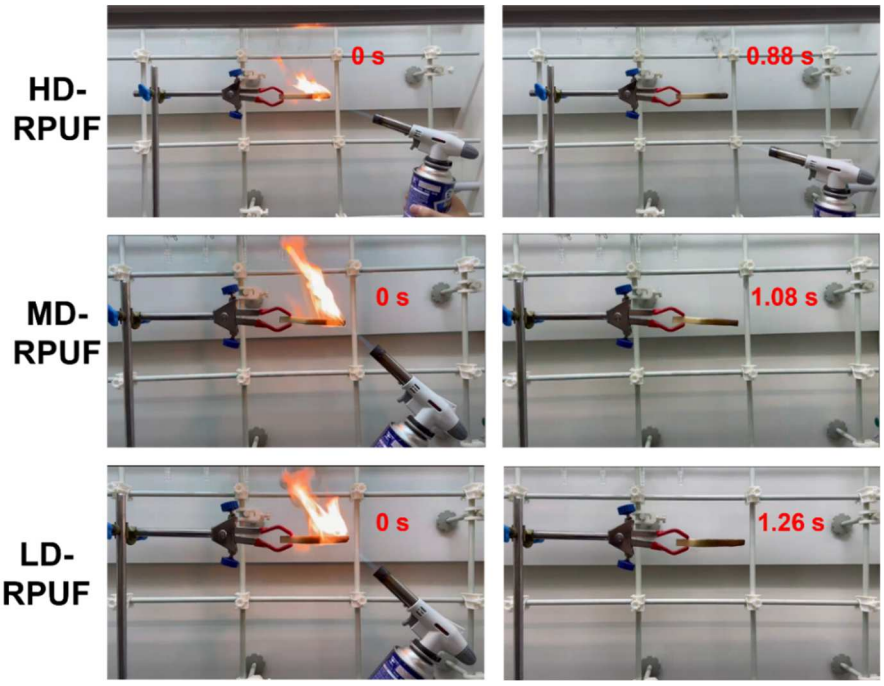

Figure 6. Flame-retardant performances of LD-RPUF, MD-RPUF and HD-RPUF.

4. Conclusions

This study introduced a novel class of rigid polyurethane foams formulated with phosphonate compounds as the flame retardant. These foams were synthesized through a standard polycondensation reaction involving dihydroxy PEG and MDI. The structures and morphologies of

these polyurethane foams were characterized using FTIR and SEM. By modulating the water content, the density and size of cells could be adjusted. These foams exhibit robust mechanical properties, characterized by a compression stress of 6.89 MPa and a tensile stress of 1.37 MPa; unique thermal stability, indicated by $T_{5\%} > 185$ °C; and excellent flame retardancy, marked by a flame extinction time of <2 s. More importantly, the predicted service lifetime for these polyurethane foams is 66 years, exceeding the standard of service lifetime of 30 years for conventional spent fuel transportation casks. This study provides a simple method for creating rigid, lightweight, and vibration-resistant soft materials suitable for the manufacture of spent fuel transport casks.

Author Contributions: Conceptualization, G.Y. and X.Z.; methodology, Z.Z.; validation, G.S., L.Y. and H.F.; formal analysis, Z.Z., L.Y. and X.C.; investigation, Z.Z., G.S. and F.Q.; resources, H.F. and X.C; writing—original draft preparation, Z.Z.; writing—review and editing, R.L., F.Q. and X.Z.; visualization, R.L.; supervision, G.Y. and X.Z.; project administration, G.Y. and X.Z.; funding acquisition, F.Q. and X.Z. All authors have read and agreed to the published version of the manuscript.

Funding: This research received no external funding

Institutional Review Board Statement: Not applicable.

Data Availability Statement: The data presented in this study are available on request from the corresponding author.

Acknowledgments: This work was financially supported by the National Natural Science Foundation of China (NSFC: 52173205, 51973114). F.Q. thanks the support from Shanghai Pujiang Program (2022PJD070).

Conflicts of Interest: The authors declare no conflict of interest.

References

1. Sun, J.; Li, G.; Lim, M.K. China's power supply chain sustainability: an analysis of performance and technology gap. *Ann. Oper. Res.* **2020**, 1-29, doi:10.1007/s10479-020-03682-w.
2. Varma, R.; Sushil. Bridging the electricity demand and supply gap using dynamic modeling in the Indian context. *Energy Policy* **2019**, *132*, 515-535, doi:https://doi.org/10.1016/j.enpol.2019.06.014.
3. Shellenberger, M. Nuclear power: Unexpected health benefits. *Nat. Energy* **2017**, *2*, 17058, doi:10.1038/nenergy.2017.58.
4. Horvath, A.; Rachlew, E. Nuclear power in the 21st century: Challenges and possibilities. *Ambio.* **2016**, *45*, 38-49, doi:10.1007/s13280-015-0732-y.
5. Jiang, H.; Wang, J.-A.J. Spent nuclear fuel system dynamic stability under normal conditions of transportation. *Nucl. Eng. Des.* **2016**, *310*, 1-14, doi:https://doi.org/10.1016/j.nucengdes.2016.09.033.
6. Qi, Z.; Yang, Z.; Li, J.; Guo, Y.; Yang, G.; Yu, Y.; Zhang, J. The Advancement of Neutron-Shielding Materials for the Transportation and Storage of Spent Nuclear Fuel. *Materials* **2022**, *15*, 3255.
7. Tae-Man, K.; Ho-Seog, D.; Chun-Hyung, C.; Jae-Hun, K. Preliminary Shielding Analysis of the Concrete Cask for Spent Nuclear Fuel Under Dry Storage Conditions. *J. Nucl. Fuel Cycle Waste Technol.* **2017**, *15*, 391-402.
8. Li, X.; Wu, J.; Tang, C.; He, Z.; Yuan, P.; Sun, Y.; Lau, W.-m.; Zhang, K.; Mei, J.; Huang, Y. High temperature resistant polyimide/boron carbide composites for neutron radiation shielding. *Compos. Part B - Eng.* **2019**, *159*, 355-361, doi:https://doi.org/10.1016/j.compositesb.2018.10.003.
9. Kim, K.; Chung, S.; Hong, J. Performance evaluation of METAMIC neutron absorber in spent fuel storage rack. *Nucl. Eng. Technol.* **2018**, *50*, 788-793, doi:https://doi.org/10.1016/j.net.2018.01.017.
10. El-Samrah, M.G.; Tawfic, A.F.; Chidiac, S.E. Spent nuclear fuel interim dry storage; Design requirements, most common methods, and evolution: A review. *Ann. Nucl. Energy* **2021**, *160*, 108408, doi:https://doi.org/10.1016/j.anucene.2021.108408.
11. Weiner, R.F.; Ammerman, D.J. Spent fuel transportation risk assessment: transportation accident analysis. *Packag. Transp. Storage Secur. Radioactive Mater.* **2013**, *24*, 147-157, doi:10.1179/1746510914Y.0000000046.
12. Diersch, R.; Weiss, M.; Dreier, G. Investigation of the impact behaviour of wooden impact limiters. *Nucl. Eng. Des.* **1994**, *150*, 341-348, doi:https://doi.org/10.1016/0029-5493(94)90153-8.
13. Aktay, L.; Johnson, A.F.; Kröplin, B.-H. Numerical modelling of honeycomb core crush behaviour. *Eng. Fract. Mech.* **2008**, *75*, 2616-2630, doi:https://doi.org/10.1016/j.engfracmech.2007.03.008.

14. Peixinho, N.; Carvalho, O.; Areias, C.; Pinto, P.; Silva, F. Compressive properties and energy absorption of metal-polymer hybrid cellular structures. *Mater. Sci. Eng. A.* **2020**, *794*, 139921, doi:https://doi.org/10.1016/j.msea.2020.139921.
15. Ryu, J.; Lim, H.; Lee, S.-H.; Lee, J. Polymer filling behaviors and imprinting velocities with pressure variation rates in nanoimprint lithography. *Microelectron. Eng.* **2015**, *140*, 67-71, doi:https://doi.org/10.1016/j.mee.2015.05.008.
16. Wang, C.; Kilic, K.I.; Koerner, H.; Baur, J.W.; Varshney, V.; Lionti, K.; Dauskardt, R.H. Polyimide Hybrid Nanocomposites with Controlled Polymer Filling and Polymer–Matrix Interaction. *ACS Appl. Mater. Interfaces* **2022**, *14*, 28239-28246, doi:10.1021/acsami.2c02575.
17. Pearce, A.K.; O'Reilly, R.K. Polymers for Biomedical Applications: The Importance of Hydrophobicity in Directing Biological Interactions and Application Efficacy. *Biomacromolecules* **2021**, *22*, 4459-4469, doi:10.1021/acs.biomac.1c00434.
18. Cichosz, S.; Masek, A.; Zaborski, M. Polymer-based sensors: A review. *Polym. Testing* **2018**, *67*, 342-348, doi:https://doi.org/10.1016/j.polymertesting.2018.03.024.
19. Akindoyo, J.O.; Beg, M.D.H.; Ghazali, S.; Islam, M.R.; Jeyaratnam, N.; Yuvaraj, A.R. Polyurethane types, synthesis and applications – a review. *RSC Adv.* **2016**, *6*, 114453-114482, doi:10.1039/C6RA14525F.
20. Mane, J.V.; Chandra, S.; Sharma, S.; Ali, H.; Chavan, V.M.; Manjunath, B.S.; Patel, R.J. Mechanical Property Evaluation of Polyurethane Foam under Quasi-static and Dynamic Strain Rates- An Experimental Study. *Procedia. Eng.* **2017**, *173*, 726-731, doi:https://doi.org/10.1016/j.proeng.2016.12.160.
21. Brondi, C.; Di Maio, E.; Bertucelli, L.; Parenti, V.; Mosciatti, T. Competing bubble formation mechanisms in rigid polyurethane foaming. *Polymer* **2021**, *228*, 123877, doi:https://doi.org/10.1016/j.polymer.2021.123877.
22. Burgaz, E.; Kendirlioglu, C. Thermomechanical behavior and thermal stability of polyurethane rigid nanocomposite foams containing binary nanoparticle mixtures. *Polym. Testing* **2019**, *77*, 105930, doi:https://doi.org/10.1016/j.polymertesting.2019.105930.
23. Maia, L.S.; de Bomfim, A.S.C.; de Oliveira, D.M.; Pinhati, F.R.; da Conceição, M.O.T.; Barud, H.S.; Medeiros, S.A.; Rosa, D.S.; Mulinari, D.R. Tuning of renewable sponge-like polyurethane physical-chemical and morphological properties using the pullulan as a reactive filler. *J. Appl. Polym. Sci.* **2023**, *140*, e53619, doi:https://doi.org/10.1002/app.53619.
24. Scholz, P.; Wachtendorf, V.; Panne, U.; Weidner, S.M. Degradation of MDI-based polyether and polyester-polyurethanes in various environments - Effects on molecular mass and crosslinking. *Polym. Testing* **2019**, *77*, 105881, doi:https://doi.org/10.1016/j.polymertesting.2019.04.028.
25. Diaz, T.J.; Cerrutti, P.; Chiacchiarelli, L.M. In-situ thermal aging of biobased and conventional rigid polyurethane foams nanostructured with bacterial nanocellulose. *J. Appl. Polym. Sci.* **2022**, *139*, 51824, doi:https://doi.org/10.1002/app.51824.
26. Qiu, F.; Tu, C.; Chen, Y.; Shi, Y.; Song, L.; Wang, R.; Zhu, X.; Zhu, B.; Yan, D.; Han, T. Control of the Optical Properties of a Star Copolymer with a Hyperbranched Conjugated Polymer Core and Poly(ethylene glycol) Arms by Self-Assembly. *Chem. Euro. J.* **2010**, *16*, 12710-12717, doi:https://doi.org/10.1002/chem.201001084.
27. Olcay, H.; Kocak, E.D. The mechanical, thermal and sound absorption properties of flexible polyurethane foam composites reinforced with artichoke stem waste fibers. *J. Ind. Text.* **2020**, *51*, 8738S-8763S, doi:10.1177/1528083720934193.
28. Chattopadhyay, D.K.; Webster, D.C. Thermal stability and flame retardancy of polyurethanes. *Prog. Polym. Sci.* **2009**, *34*, 1068-1133, doi:https://doi.org/10.1016/j.progpolymsci.2009.06.002.
29. Ge, C.; Wang, S.; Zheng, W.; Zhai, W. Preparation of microcellular thermoplastic polyurethane (TPU) foam and its tensile property. *Polym. Eng. Sci.* **2018**, *58*, E158-E166, doi:https://doi.org/10.1002/pen.24813.
30. Son, T.W.; Lee, D.W.; Lim, S.K. Thermal and Phase Behavior of Polyurethane Based on Chain Extender, 2,2-Bis-[4-(2-hydroxyethoxy)phenyl]propane. *Polym. J.* **1999**, *31*, 563-568, doi:10.1295/polymj.31.563.
31. Li, X.; Wang, G.; Yang, C.; Zhao, J.; Zhang, A. Mechanical and EMI shielding properties of solid and microcellular TPU/nanographite composite membranes. *Polym. Testing* **2021**, *93*, 106891, doi:https://doi.org/10.1016/j.polymertesting.2020.106891.
32. Takano, M.; Takamatsu, K.; Saito, H. High-Strength Heat-Elongated Thermoplastic Polyurethane Elastomer Consisting of a Stacked Domain Structure. *Polymers* **2022**, *14*, 1470.
33. Shuai, M.-K.; Gong, Y.; Cheng, F.; Zhang, J.; Li, R.-B.; Pan, J.; Li, N.; Xu, J.-F.; Liu, X.-Q.; Yang, X.-L.; et al. Innovation in lifetime prediction of rigid polyurethane foam through random vibration and comparison

with conventional methods. *Polym. Testing* **2023**, *125*, 108122, doi:https://doi.org/10.1016/j.polymertesting.2023.108122.
34. Doyle, C.D. Kinetic analysis of thermogravimetric data. *J. Appl. Polym. Sci.* **1961**, *5*, 285-292, doi:https://doi.org/10.1002/app.1961.070051506.
35. Gong, Y.; Tang, J.; Sun, B.-N.; Yang, Z.-G.; Shi, X.-Q.; Liu, X.-Q.; Xie, Y.-C.; Xu, X.-L. Comparative study on different methods for determination of activation energies of nuclear cable materials. *Polym. Testing* **2018**, *70*, 81-91, doi:https://doi.org/10.1016/j.polymertesting.2018.06.029.
36. Zeng, F.; Men, X.; Chen, M.; Liu, B.; Han, Q.; Huang, S.; Zhao, H.; Wang, Y. Molecular-micron multiscale toughening and flame retarding for polyurethane foams. *Chem. Eng. J.* **2023**, *454*, 140023, doi:https://doi.org/10.1016/j.cej.2022.140023.